

# Chapter 8

## The Effect of Zeolitic Imidazole Framework-8@Graphene Oxide on the Performance of Polymeric Membranes Used for Wasterwater Treatment



T. A. Makhetha and R. M. Moutloali

**Abstract** The practice of using zeolitic imidazole framework-8@graphene oxide (ZIF-8@GO) is increasing tremendously in membrane technology for wastewater treatment. This is not only due to the limitations posed by ZIF-8 or GO when used separately, but because of the interesting properties a composite of these materials (ZIF-8@GO) possesses, such as hydrothermal stability, porosity, crystallinity, hydrophilicity, and selectivity. Therefore, it is necessary to expand knowledge on the overall properties of the resultant ZIF-8@GO as well as the ZIF-8@GO incorporated into polymeric membranes. This chapter covers the literature on recent developments on ZIF-8@GO incorporated into polymeric membranes for wastewater treatment. The focus is on the morphological features, thermal and chemical stability, membrane performances i.e., rejection of pollutants from wastewater, water flux, selectivity as well as antifouling and or antibiofouling properties of these ZIF-8@GO embedded in polymeric membranes.

### 8.1 Introduction

Each person has the right to adequate, perpetual, accessible, safe, and cheap water for personal and domestic use. However, not everyone in the world has access to safe and readily available water [81, 86, 94]. It is worth noting that having clean and safe water can greatly boost every country's economy and significantly reduce

---

T. A. Makhetha

Department of Chemical Sciences, University of Johannesburg, Doornfontein, Johannesburg 2028, South Africa

R. M. Moutloali (✉)

Institute for Nanotechnology and Water Sustainability, College of Science, Engineering and Technology, University of South Africa, Florida Science Campus Florida, Johannesburg 1709, South Africa

e-mail: [moutlr@unisa.ac.za](mailto:moutlr@unisa.ac.za)

poverty, especially in African countries [86, 94]. Nonetheless, different factors such as increasing water scarcity, climate change, urbanization, population growth, and demographic changes have been identified to pose challenges to water supply systems [44, 46, 49]. As a result of these challenges, World Health Organisation (WHO) stated that, by 2025, half of the world's population would be living in water-stressed areas [99]. Consequently, there is a need to review and scrutinize the already existing membrane processes that are used for wastewater treatment for reuse to ensure the WHO projections are inappropriate.

Membrane processes such as reverse osmosis (R.O.), nanofiltration (N.F.), ultrafiltration (U.F.), and microfiltration have been extensively utilised for wastewater treatment due to their ease of preparation and operation, are cost-effective and possess high efficacy [20, 32, 44, 46, 49, 99]. However, these membrane technologies are hamstrung by their perceived high energy demands or chemical intensiveness during preparation and high fouling tendency, thus requiring frequent backwashing or cleaning [20, 32, 44, 99]. Furthermore, membrane fouling is considered as the number one drawback hindering the widespread adoption and use of membrane processes in wastewater treatment [44, 46, 49]. In definition, membrane fouling results from the deposition on the membrane surface or adsorption of organic filth such as proteins, natural organic matters, and humic substances as well as microorganisms [22]. It is worth noting that membrane fouling, caused by either bio or organic deposition, is highly affected by the membrane properties and characteristics that greatly dictate its application and performance [22]. In addition, there are other factors that play a crucial role in membrane fouling, i.e., the pH of the feed solution, the concentration of the solute in the feed, and the structure of the membrane [76]. Mitigation strategies to minimize fouling have resulted in the development of modified polymeric membranes leading to improved membrane performances and application.

The incorporation of porous and/or hydrophilic materials into polymeric membranes is currently considered one of the most effective ways to achieve functional membranes for wastewater treatment [32, 44, 46, 49, 58]. Consequently, intensive studies and reports dedicated to the utilisation of metal organic frameworks (MOFs) in membrane formulation due to their controllable pore aperture, pore size, diverse structures, morphologies, and their tunable functionalities [13, 14, 20]. These studies revealed that understanding key features of MOFs and how these interact with polymeric membrane matrices could ensure the production of defect-free MOF-integrated membranes for the filtration process [3]. It is worth noting that not all MOFs are water stable and compatible with the polymers utilized in membrane technology for wastewater treatment [3, 14, 44, 46, 49]. This has led to carbon-based material such as graphene oxide (GO) being used as a dispersant for MOFs as well as to enhance the water stability of the MOFs [11, 43, 47, 55, 57, 69, 89]. GO is a 2D carbon material with oxygenated functional groups, such as carboxyl, hydroxyl, and epoxy, contained on its edge and on the basal plane [53]. These functional groups bestow GO with good hydrophilicity. Furthermore, the oxygenated functional groups make GO reactive, making its surface modification easier and hence used to anchor MOFs increasing their compatibility with the polymer matrix [53, 103].

Wang et al. [11] fabricated an electrospun membrane from polylactic acid (PLA) polymer modified with ZIF-8@GO filler for methylene blue (MB) adsorption and its photodegradation from wastewater. An increase in hydrophilicity and enhanced mechanical strength of the polymer matrix was observed with the incorporation of the ZIF-8@GO filler. The resultant PLA/ZIF@GO composite membranes exhibited enhanced adsorption capacity and photocatalytic efficacy for MB compared to Zhang et al., which rejected only 50% of methyl blue using ZIF-8/HPEI hybrid filler modified PAN [97].

On the other hand, Wang and co-workers [89] investigated the effect of ZIF-8@GO on the antibacterial performances of thin-film composite membranes. The authors found that the increasing ZIF-8@GO content enhanced the antimicrobial properties of the thin film composite membranes. Furthermore, it was also reported that a synergistic effect of the hydrophilic GO and porous ZIF-8 improved the permeability of the thin film composite membranes without compromising on their solute rejection properties. A similar positive contribution resulting from the incorporation of ZIF-8@GO composite fillers on hydrophilicity, water flux, dye rejection as well as fouling resistance in ultrafiltration membrane was reported by [97]. Furthermore, we also reported on how the antibiofouling membrane properties were enhanced by the incorporation of ZIF-8@GO encapsulating the well-known antimicrobial agents, viz. silver and copper nanoparticles [57].

The chapter summarises recent progress on MOFs@GO composite and its use to modify polymeric membranes for wastewater treatment. The focus is on the impact of ZIF-8@GO on structural and morphological features of the resultant membranes; i.e., membrane pore size or shape, surface roughness, and hydrophilicity and their influence on the membrane performance parameters such as water flux/permeability, solute rejection mechanisms, and the effect of the composites on membrane fouling.

## 8.2 General Description of Metal–Organic Framework (MOFs)

Metal–organic frameworks (MOFs) are classified as both organic and inorganic materials due to their constituents, i.e., transition metal cations (such as Co, Zn, Zr, and Cu) and multidentate organic linker (such as terephthalic acid and 2-methylimidazole) [36]. The formation of MOFs is through the coordination of the metal clusters with the functional groups from the ligand/linker; hence they are also called porous coordination frameworks [35]. MOFs have interesting features such as a high surface area with their porosity and pore sizes much greater than those of molecular sieve materials that can be controlled or tuned from micro to mesoporous by simple methods [12, 32, 44, 46, 49, 99].

MOFs are divided into different categories based on their metal clusters and the linker used. More insight on the differences in MOFs is presented in the sections below. Thus far, there is isorecticular metal–organic frameworks (IRMOFs) [6, 30,

54, 70, 84, 96], zeolitic imidazolate frameworks (ZIFs) [4, 5, 7, 59, 65], materials of institute lavoisier frameworks (MILs) [10, 15, 16, 18, 30, 60, 61, 67], University of Oslo (UiO) [8, 34, 51, 93], etc. New types of MOFs are being developed, looking at using lanthanides and actinides metals with different linkers [28, 78]. The f-orbital lanthanides and actinides are less available for bonding which results in big particle size in comparison to the d-orbital transition metals [78]. Furthermore, due to less available bonding sites, the lanthanides metal center forms the first coordination sphere that constitutes the primary building units (PBU) of the lanthanide MOFs. The PBU then combines into larger, unique polymeric subunits that are repeated throughout the entire framework that is known as the secondary building unit (SBU) [28]. Subsequently, these lanthanides and actinides MOFs provide enhanced catalytic binding sites compared to the transition metal MOFs [28].

### 8.2.1 Isoreticular Metal–Organic Frameworks (IRMOFs)

Isoreticular MOFs are the ones from organic ligands of different sizes, but with a common symmetry/geometry resulting to MOFs of related topologies, but with expanded pore sizes and volumes [73]. IRMOFs series have similar primitive cubic packing (pcu) topology and can be fabricated from MO–C clusters where M is a metal and different ligands as demonstrated in Fig. 8.1 [6, 30, 54, 70, 84, 96]. The varied ligand result to change in surface area, physical and chemical properties; hence these are used for various applications such as gas adsorption, catalysis, and sensors

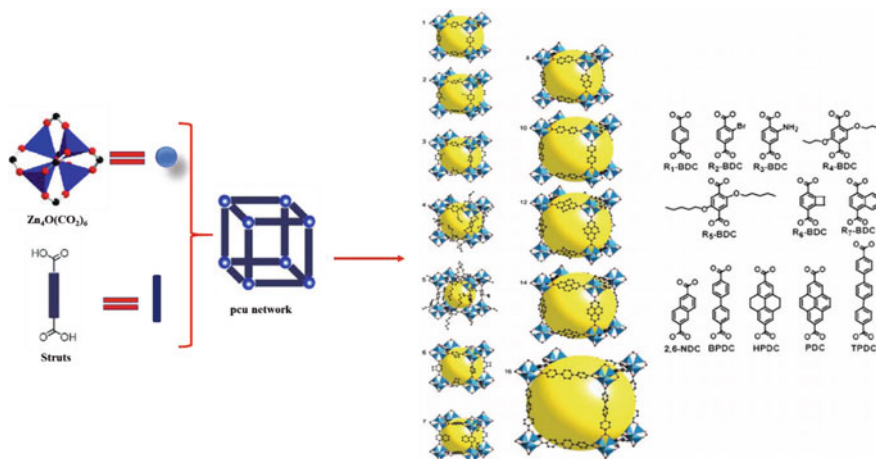


**Fig. 8.1** Description of the formation of IRMOFs and structural representation of IRMOFs and the structure of the ligand derivatives of IRMOFs family. Yellow central sphere represents open pore spaces. Reproduced with permission from [96] and [70]. Copyright 2012, Royal Society of Chemistry and 2014, Springer-Verlag Berlin Heidelberg

[6, 30, 54, 70, 84, 96]. However, IRMOFs are not applicable in water research since they easily degrade in a humid environment even at room temperature due to the rupture of the bond between a metal atom and the central oxygen from the metal cluster [6]. The molecular length and breadth of the organic ligand control the size of the cavities (yellow spheres) of the resultant MOFs.

## 8.2.2 Zeolitic Imidazolate Frameworks (ZIFs)

Extensive research has been done on MOFs in the past decades, which led to the development of the subfamily zeolitic imidazolate frameworks (ZIFs) [4, 5, 7, 59, 65]. The main constituents of ZIFs are the two transition metals, i.e., zinc and cobalt, and a range of imidazolate linkers coordinated in a tetrahedral shape that is similar to that in crystalline aluminosilicate zeolite and hence their generic name (Fig. 8.2) [59]. The coordination of ZIFs is built from M–I.M–M (M = tetrahedrally coordinated metal ion, I.M. = imidazolate, and its derivative) bonding with a M–I.M.–M angle of  $145^\circ$ , which is similar to the Si–O–Si angle in zeolites (Fig. 8.3) [4, 7, 59]. Interestingly with ZIFs, their structure depends primarily on the type of solvent used and the linker imidazolate (Fig. 8.4) [4, 5, 7, 59, 65]. It has been observed that when the functionalized linkers are used, greater structural diversity in ZIFs is possible. Similarly, ZIFs are thermally and chemically stable; moreover, ZIFs have been shown to be water stable in comparison to other MOFs [4, 5, 7, 59, 65]. This is due to the strong metal to nitrogen bond that shows intensive resistance to alkali water and organic solvents [3]. Furthermore, ZIFs are hydrophobic; therefore, water molecules

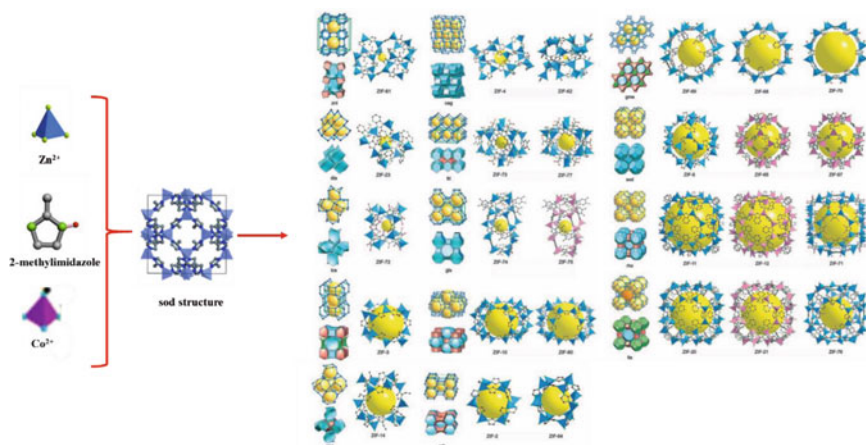


**Fig. 8.2** Representation of assembly of different types of ZIFs and their respective topologies. Yellow central sphere represents open pore spaces. Reproduced with permission from [5]. Copyright 2008, American Association for the Advancement of Science

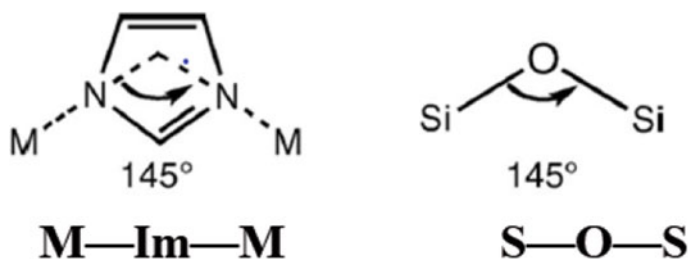


**Fig. 8.3** General structural model of ZIFs showing angle similarities with the aluminosilicate zeolites. Reproduced with permission from [59]. Copyright 2020, Taylor & Francis Online

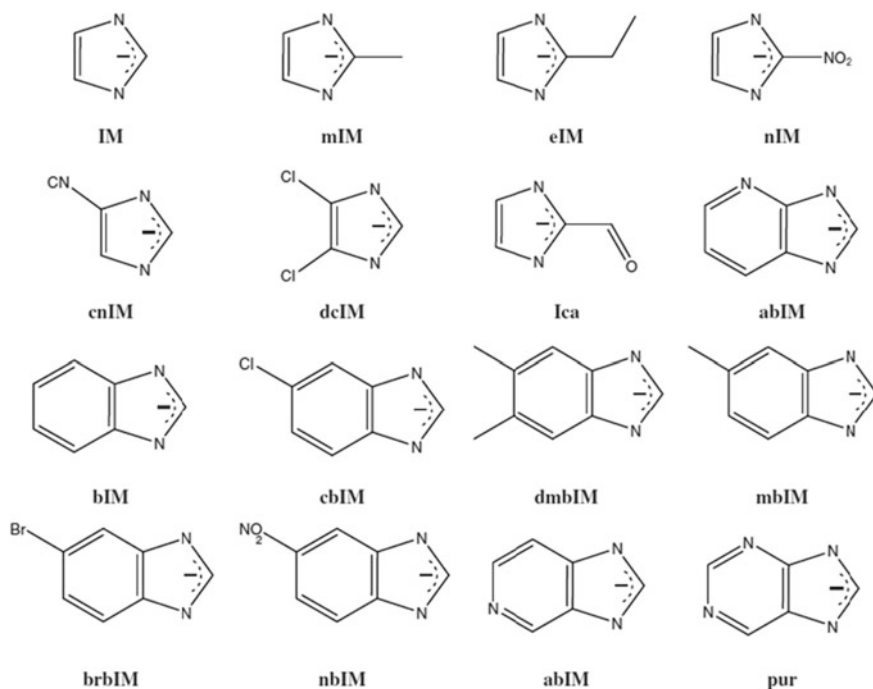


**Fig. 8.4** Different types of imidazole ligands used for the synthesis of ZIFs. Reproduced with permission from [7]. Copyright 2014, Springer Nature Switzerland AG

cannot penetrate through the framework pores to destroy their structure [59]. ZIFs have been widely applied in gas storage/separation, catalysis and recently in water purification and wastewater treatment [4, 5, 7, 59, 65].

### 8.2.3 Materials of Institute Lavoisier Frameworks (MILs)

MILs were firstly discovered in 2000 by Millange and Serre et al. [18]. These types of MOFs are formed from the chemically inert metals such as Cr, Fe, Sc, V, Al, Ti, Ni, and Mn. and the benzene-1,4-dicarboxylate linkers (Fig. 8.5) [10, 15, 16, 18, 30, 60, 61, 67]. The structure of MILs is made by coordinating benzene-1,4-dicarboxylate ligands metal centres that are octahedrally connected and share trans-corners to give infinite, linear inorganic chains [10, 15, 16, 18, 30, 60, 61, 67]. This yields an open structure with diamond-shaped channels running parallel to the inorganic chains, as presented in Fig. 8.6. MILs are known for their flexibility which allows them to expand and contract when exposed to stimuli such as pH change, temperature, the introduction of guest molecules, and pressure without any change in their crystalline structure [10, 15, 16, 18, 60, 61, 67]. Such MOFs have been used in various applications such as catalysis, sensing, drug delivery and degradation or capture of pollutants [10, 15, 16, 18, 60, 61, 67].

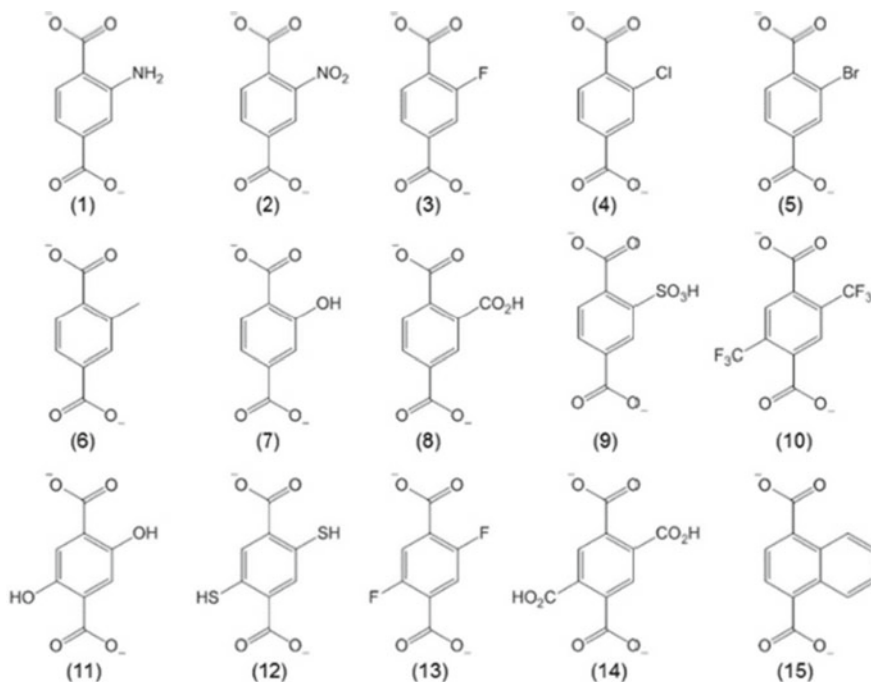


**Fig. 8.5** Different types of ligands used to synthesize MILs. Reproduced with permission from [82]. Copyright 2020, John Wiley and Sons



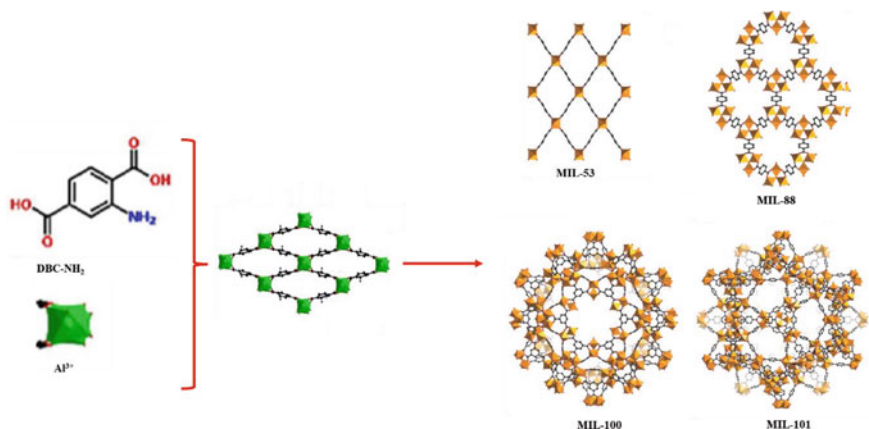


**Fig. 8.6** Representation of assembly of different MILs. Reproduced with permission from [91]. Copyright 2020, Royal Society of Chemistry

### 8.2.4 University of Oslo (UiO)

UiO-66 MOF was first synthesized at the University of Oslo and hence its name. Similar to other MOFs such as MILs, UiO-66 is formed when the 1,4-benzenedicarboxylate organic linkers coordinate to Zr metal ions in clusters contained as  $Zr_6O_4(OH)_4$  nodes (Fig. 8.7) that are different to that of MILs [8, 34, 51, 93]. UiO-66 MOFs present an octahedron shape and are known to be stable in acids and water vapor, and are thermally stable [93]. As such, they have been widely used in aqueous applications such as dye adsorption and pervaporation [20].

### 8.2.5 Summary of MOFs

From the general description of MOFs, it is evident that not all MOFs are suitable for water application without modification. Therefore, some factors need to be considered when choosing MOFs to be used in water-related applications. It is also worth noting that the structure and the morphology of the MOFs are not only dependent on the building blocks and the linker used, as shown in Figs. 8.1, 8.3, 8.5 and 8.7. In essence, some factors such as temperature, compositional parameters (i.e., pH, type of salt and molar ratio), and solvent influence the structure and the morphology of MOFs [3]. For example: during the synthesis of MOFs, usually, the solvents are not incorporated within the framework; however, they might direct the crystal growth of the MOFs by acting as directing agents [29, 42, 74]. Furthermore, the nucleation growth of MOFs can be increased, which then results in a smaller particle size of MOFs by using more reactive metal precursors, i.e., using  $Zn(NO_3)_2$  instead of using  $ZnSO_4$  [102].



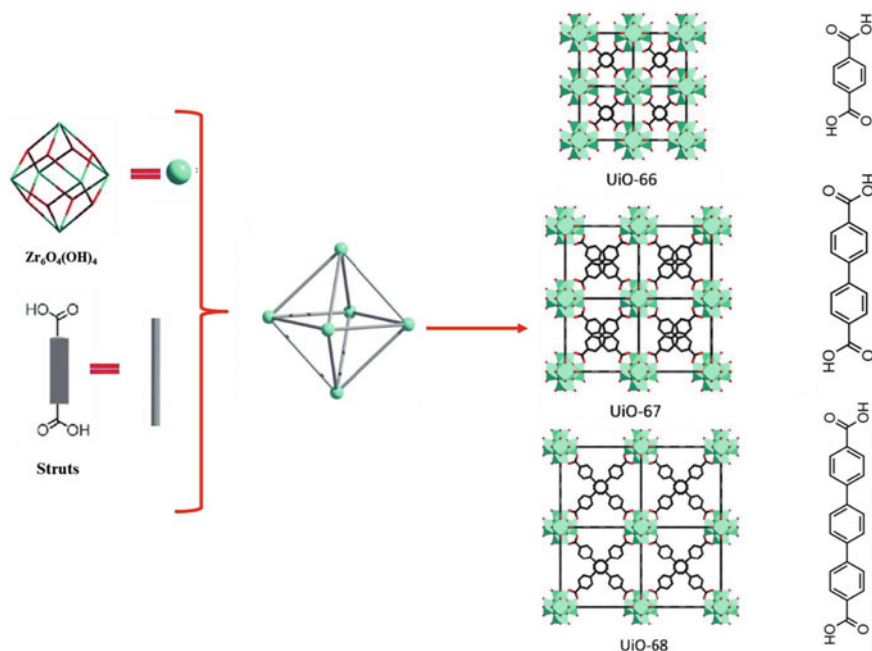


**Fig. 8.7** Representation of assembly of different UiO-66 MOFs. Reproduced with permission from [105]. Copyright 2018 John Wiley and Sons

Additionally, the molar ratio between the linkers and the metals does play a huge role; the excess of the linker might slow down the growth rate as it will function as a stabilizing agent [52, 74]. Another important factor to consider is high temperatures used for the synthesis of MOFs since excessively high synthesis temperature may oxidize metal ions [74]. Thus, MOFs are recently used as precursors for metal oxides [71]. Finally, the addition of additives such as trimethylamine (TEA) and cetyltrimethylammonium bromide (CTAB) might affect the growth rate resulting in smaller particle sizes [25, 66].

### 8.3 Factors to Consider When Choosing MOFs in Water Application

#### 8.3.1 MOFs Should Have High Water Stability

MOFs need to be water stable for them to be applied in water research, such as in membrane technology for water treatment and purification. Most MOFs, such as isorecticular MOF-5 and HKUST (Hong Kong University of Science and

Technology), a metal–organic framework made up of copper nodes with 1,3,5-benzenetricarboxylic acid struts between them, are susceptible to moisture and hydrolyze, resulting in decomposition and displacement of the building block leading to a loss of crystallinity and porosity of MOFs [6]. As a result, only a handful of MOFs are stable in water without any modification. These include MOFs with high valence metal ions such as  $Zr^{4+}$ ,  $Ti^{4+}$ ,  $Cr^{3+}$ , and  $Fe^{3+}$  coordinated to ligands shown in Figs. 8.6 and 8.7, these include MOFs such as MILs and UiO [34, 60, 67, 93]. Their stability is due to the charge density of these high valence metals that is related to their corresponding ionic radius. In this case, the stability of MOFs is enhanced since the smaller the effective ionic radius is linked to the high charge density of the metal ion [3].

Other water-stable MOFs are those synthesized using azolate based organic ligands such as imidazoles, pyrazoles, triazoles, and tetrazoles (Fig. 8.4) [5, 59, 65]. The stability of the azolate ligands is ascribed to their higher pKa values [45]. This results in the stability of the ligands being maintained even though low valence metal ions are used, e.g., Zn in ZIF-8 is one of the perfect examples [59]. Furthermore, the strong bond formed between metal-nitrogen is maintained, resulting in higher water stability of the ZIFs [5].

Modification of MOFs with specific functional groups can prevent water molecules from entering into their framework structure. For instance, the introduction of the hydrophobic functional groups such as methyl groups and non-polar alkyl groups enhances water stability of the resultant MOFs [45]. Consequently, hydrophobic pore surfaces and encapsulated metal ions provide steric hindrance as a mechanism that blocks water from seeping into the frameworks. Ultimately the exclusion of water molecules in the framework structure imparts and enhances the water stability of MOFs.

Finally, the formulation of the core–shell MOFs does play a crucial role in enhancing the water stability of the MOFs. In this case, the water-stable MOFs act as a shell that protects the water-sensitive core [3, 45]. Most interestingly, MOFs@MOFs materials offer a synergistic effect, and new properties are often realized in these types of materials [44, 46, 49, 68, 95]. In adsorption and separation application, MOFs@MOFs materials are fabricated from MOFs with different apertures in order to serve as molecular sieves [95]. As such, the MOF with a larger opening will act as a cargo transport highway, while the MOF with a smaller opening will act as a filter [95].

Furthermore, these MOFs@MOFs materials are synthesized using different synthesis routes, i.e., epitaxial growth, post-modification, and one-pot synthesis for MOFs@MOFs materials [44, 46, 49, 68, 95]. These synthesis routes offer different structural features as well as different properties that can be utilized for different applications [95]. In definition, epitaxial growth is the seeding/growing of one MOFs on the surface of the other MOF through seed-mediated synthesis, e.g., growth of ZIF-8@ZIF-67 or vice versa [44, 46, 49, 68, 95]. On the other hand, a post modification route is the most flexible method for the synthesis of MOFs@MOFs materials, wherein, different strategies are employed such as Ostwald ripening-mediated

method, selective trans-metalation method, internal extended growth method, post-synthetic ligand exchange, retrosynthetic design, and surfactant-mediated overgrowth method [95]. Finally, in the one-pot synthesis method, the metal ions and ligands of the inner and outer MOFs are added into the reaction system simultaneously [95]. Nonetheless, the porosity of MOFs@MOFs materials is of paramount, especially in separation application.

### 8.3.2 Suitable Pore Size for MOFs Appropriate for Use in Membrane Technology

MOFs have a high controllable level of porosity that makes them suitable to be used in all membrane types, i.e., reverse osmosis, nanofiltration, ultrafiltration, and microfiltration membranes [20]. In these cases, the aperture of their cages and the pore sizes play a crucial role in the membrane process resulting in enhanced water flux by providing alternative water pathways, decreasing water resistance, and reducing tortuosity (Fig. 8.8) [39]. The pore size of the MOFs does affect the rejection of pollutants; small pore size and aperture cage are mostly preferred to allow water transport while preventing transport of dissolved ions across the membrane [14]. As such, the appropriate pore or cavity size of the MOFs in membrane technology is the small pore size that can only allow water molecules while preventing other small dissolved salts; this is referred to as molecular sieving. In a case where the pore size of the MOF is big enough to allow pollutants within the pores, there is an interaction of the pollutants with the adjacent surfaces of the MOF; hence adsorptions will take place within the MOF cavities [44, 46, 49]. The selection of the pore size does also

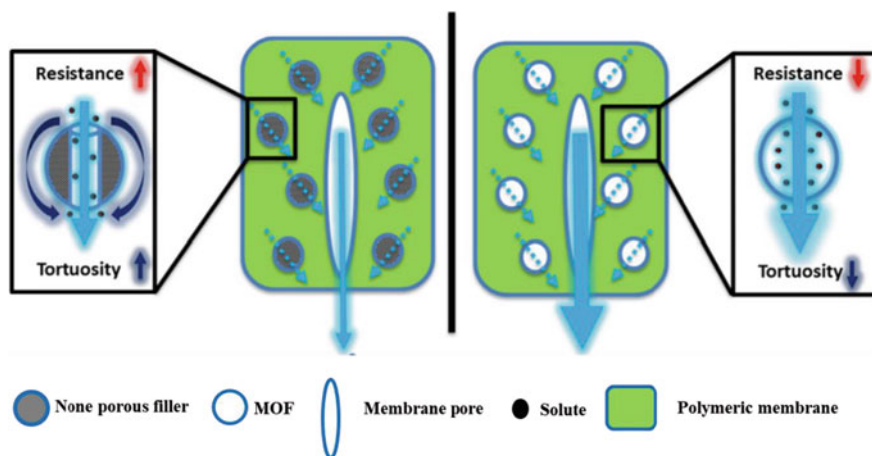


**Fig. 8.8** Representation of the water transport through the macropores inside the MOF incorporated into polymeric membrane. Reproduced with permission from [39]. Copyright 2015 Elsevier

depend on the targeted pollutant, similarly in gas separation since gas molecules are different in size [44, 46, 49].

### ***8.3.3 Importance of Uniform Dispersibility of Fillers in Composite Membranes***

Free-standing layers of MOFs with uniform pore size and high level of porosity can be used to ensure consistent properties throughout MOF membranes [44, 46, 49]. However, these membranes can barely be approved for practical application due to their poor mechanical strength. Therefore, MOFs incorporated into membranes are widely used and approved [3, 43, 47, 99]. As such, MOFs are generally used as nanofillers, and the dispersion of MOFs crystallites plays an important role in the performance of the composite membranes [3, 43, 47, 99]. The concentration or loading of MOF nanofillers below 5 wt.% is the most appropriate quantities to use for resulting in uniform dispersion in the membrane matrices (Kadhom and Deng, 2018b). However, MOFs are not entirely compatible with most polymer matrices. Hence, in other instances, a compatibilizer or a dispersant such as carbonaceous materials (graphene oxide, carbon nanotubes) play a crucial role in properly dispersing MOFs in a matrix [41, 106]. As the concentration of the MOF nanofillers increases, the surface energy of the MOF particles is reduced as a result of high surface energy that is caused by Van der Waals forces (Manuscript et al., no date), leading to agglomeration. Poor dispersion compromises the mechanical properties of the membranes resulting in poor membrane performances [41, 106]. Furthermore, a high concentration of MOF filler may result in changes in the rheology of the membrane matrix affecting the physical and chemical properties of the resultant membrane, as a result, decreasing membrane performances such as water flux, rejection as well as fouling resistance. (Manuscript et al., no date). Consequently, there is a need to investigate different strategies to employ to improve the MOF/polymer interface.

So far, a great number of approaches have been used to improve MOF/polymer interface, such as using different methods for preparing the dope solution, surface modification of the MOFs or the polymer, adding interface agents, i.e., ionic liquids, and using MOF composites, i.e., MOF@GO [48]. Most of these approaches have shown interesting results; however, there is still more to be done to improve the interfacial voids found between the MOF and the polymer [48]. However, few interfacial voids and better MOF/polymer interactions have been reported for MOF composites due to better compatibility between the GO and most polymers [55, 57, 43, 47, 87, 106].

## 8.4 ZIF-8@GO Fillers Used in Membrane Technology for Wastewater Treatment

MOFs have been used as fillers in membrane technology for wastewater treatment [27]. However, MOFs as inorganic fillers are incompatible with organic polymer matrix, which has led to the use of hybrid fillers that emanated from the concern of poor dispersion of the inorganic filler in the organic polymeric membrane. Consequently, the use of carbonaceous materials as compatibilizers or dispersants has proven to be very crucial [11, 89]. It is worth noting that, in most cases, the composite membrane will exhibit both the properties of the individual materials used to form the hybrid filler [11, 56, 57, 89]. Interestingly, in membrane technology, the filler material improves the properties of the resultant composite membrane; these include the physico-chemical, i.e., improved surface morphology, enhanced thermal stability, improved mechanical properties, improved membrane performance, i.e., water flux, rejection, and fouling resistance. Therefore, understanding the individual properties of the materials such as MOFs and GO as well as the resultant composite is crucial as it provides insight into how the morphology and/ or structure of the resultant composite membranes can be influenced, leading to better membrane performance.

### 8.4.1 Morphology

There are three different groups of membranes, i.e., biological membranes, artificial membranes, and theoretical membranes [72]. This chapter focuses on artificial membranes such as R.O., NF, U.F., and M.F. with asymmetric structure mostly used in industries [72]. A typical asymmetric membrane structure is shown in Fig. 8.9 and consists of two layers that can be viewed from its cross-section. This type of membrane consists of a top dense thin layer usually referred to as the top skin layer, and a bottom porous sublayer [62, 72]. These two layers play a crucial role. The dense top layer controls the performance, such as the permeation properties and water flux of the membrane. The porous sublayer only provides mechanical strength to the membrane. On the other hand, the membranes with symmetric structures do not possess top dense or porous bottom layers and are uniform throughout (Fig. 8.9). There are two types of asymmetric membranes, (1) an *integrally skinned* asymmetric membrane where the material of the top layer and porous sublayer is the same [19]. (2) The composite membrane where the polymer of the top skin layer is different from the polymer of the porous sublayer [19]. Interestingly, the porous sublayer can be modified separately to optimize the overall performances of the membrane in comparison to the integrally skinned asymmetric membrane [19, 72]. For example, the porous layer can be optimized by choosing the amount of the polymer used that affects the viscosity of the casting solution, as a result affecting the exchange rate of water and solvent. The addition of the pore former, e.g., poly(vinyl pyrrolidone) is

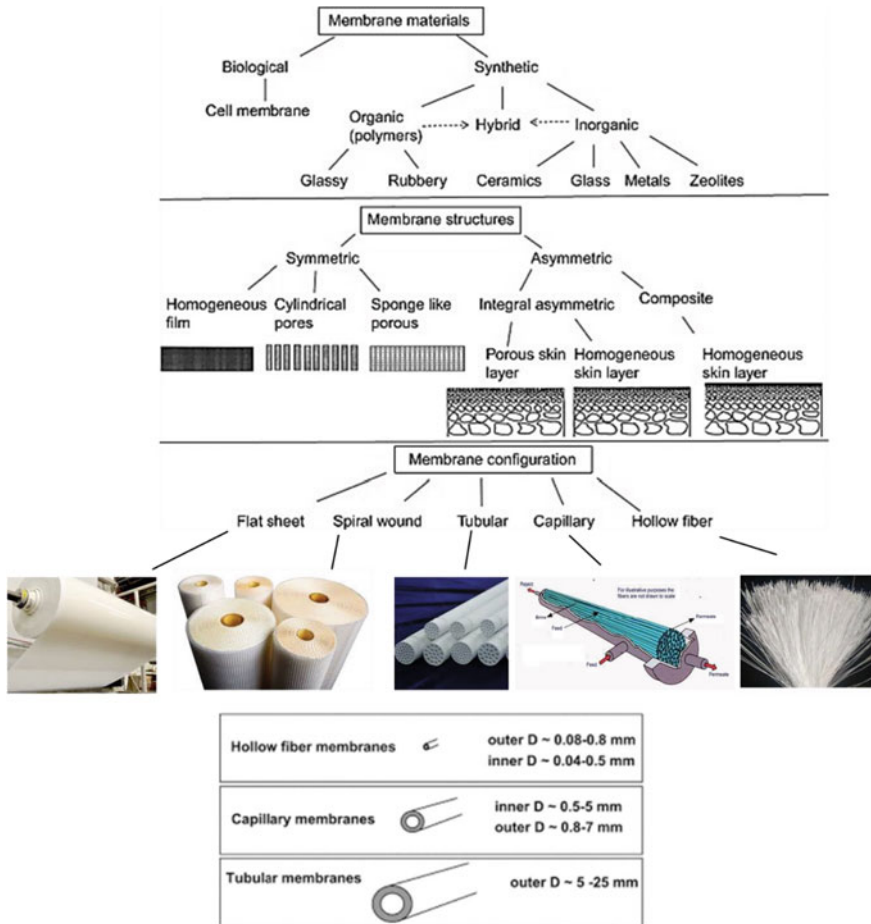


**Fig. 8.9** Classification of membranes based on materials of construction, structural attributes, configuration and diameter of the configuration. Reproduced with permission from [19]. Copyright 2019 Elsevier

also used to optimize the porous layer [41]. The top layer can be modified by understanding the effects and the amount of the monomers that are used to fabricate the top layer (W J [37, 38]). For example, m-phenylenediamine (MPD) aromatic diamine and trimesoyl chloride (TMC) acid chloride have proven to be the most successful monomers for the fabrication of the top layer of the composite membrane (W J [37, 38]).

The properties of membrane pore structures, such as pore size, pore size distribution, pore density, surface roughness, etc., are the backbone of the membrane processes since such properties control the filtration characteristics of membranes [19, 62, 72]. Membrane preparation protocols that are geared towards controlling the physical properties like pore size and pore size distributions of the membranes

are continuously being developed. These include the phase inversion method that is divided into four different main types (i.e., non-solvent-induced phase separation (NIPS), vapor induced phase separation (VIPS), thermally induced phase separation (TIPS), and solvent evaporation-induced phase separation (SEIPS)). NIPS, TIPS, and VIPS are extensively used for producing polymer membranes, whereas SEIPS involves the use of liquid monomers for the production of membranes [21, 83]. The difference between these methods is the mechanism in which the phase inversion process occurs [83]. Wherein TIPS method uses high temperatures to prepare a dope polymer solution thereafter cooled to induce phase separation followed by polymer solidification [50, 83]. On the other hand, in NIPS, a homogeneous solution of the polymer and the solvent is cast on a glass plate and subsequently submerged into a coagulation bath containing a non-solvent, e.g., deionized water; hence, precipitation occurs due to the exchange of solvent into non-solvent [21, 55]. In contrast to NIPS and TIPS, the phase inversion processes in the VIPS method occur in the open air under-regulated humidity [64].

There are fundamental factors that affect the phase inversion process in membrane formation when using NIPS, TIPS, and VIPS methods, these include the choice of solvent-nonsolvent system, the composition of the coagulation bath, the composition of the polymer solution, and film casting conditions [21, 83]. As such, the desired membrane is achieved by optimizing the above-mentioned factors. Furthermore, additives, such as organic, i.e., poly(vinyl pyrrolidone) and poly(ethylene glycol), as well as inorganic additives, i.e., nanoparticles, are often used as a third component during membrane formation [21, 83]. These additives are often utilized to regulate membrane pore formation, pore structure, pore distribution, and chemical properties, which then influence the membrane performance as well as the membrane application [21, 64, 83]. There are numerous techniques that are utilized to assess the effectiveness of these various factors in membranes formation. For example, Younas and co-workers investigated the effect of coagulation residents on the morphology, mechanical properties as well as gas transport behavior of the resultant membranes [50]. The findings revealed that the pores increased with increased exposure of the membranes in the coagulation bath, which allowed enough time for de-mixing to occur. Furthermore, it was realized that an increase in pore density resulted in a thin dense layer that positively influenced the resistance of the membranes towards gas transport [50].

The usage of several techniques to determine pore size and distribution characteristics of the membranes include the mercury porosimetry, permoporometry, bubble point method, thermoporometry, and the adsorption method, as well as methods based on liquid or gas transport, microscopic methods such as scanning electron microscopy (SEM), transmission electron microscopy (TEM), and atomic force microscopy (AFM) are commonplace [62, 72]. Herein, the focus will be limited to the microscopic methods, i.e., SEM and AFM. These two techniques are of interest in this chapter since they provide a clear and visual morphological insight with respect to pore size, pore density, pore distribution, as well as surface roughness. Moreover, each technique can provide more than a single information about the characteristics



of the membrane pore, and the results obtained are independent of the other parameters unlike the other mentioned techniques. Whereas, in other techniques such as the bubble point technique and porosimetry, only the radius of the largest pore is determined, and the results depend mostly on the contact angle as well as the surface tension of the membrane [85].

#### 8.4.1.1 Sem

SEM is an electron microscope that uses a focused beam of electrons that react with the sample to produce a topological image. In membranes, a top surface and a cross-section are usually investigated where the top surface reveals the surface pores of the membranes. SEM usually underestimates pore diameters due to the metal coating that is necessary to increase conductivity [31]. The measured pore diameter value varies with the coating rate, coating period, and pore shape [31, 62]. It is worth noting that the pore shape is usually not cylindrical but funnel-shaped, so the coating can reduce the pore size leading to underestimation of the actual size [72]. The structural changes/defects may also occur due to the damage by the electron beam or by the requirement to operate in a high vacuum [72]. Nonetheless, SEM is widely used in membrane technology to assess the topography of the membrane.

The effect of ZIF-8@GO fillers on membrane topography is dependent on the membrane fabrication protocol used. For instance, its effects on membranes formed using phase inversion for U.F. membranes are different from that obtained using interfacial polymerization process for N.F. and R.O. membranes. For instance, in the phase inversion process, ZIF-8@GO filler affects the rate at which the de-mixing process occurs therefore impacting/influencing the membrane pore size, pore distribution, and the shape of the pores that are formed [19, 72]. For example, we observed a decrease in membrane pore size but an increase in pore density and pore distribution as the amount of ZIF-8@GO composite in the PES composite membranes was increased in comparison to pristine PES membrane [56]. Furthermore, the cross-section of the composite membranes demonstrated a formation of a sponge-like membrane compared to the pristine membrane at higher ZIF-8@GO loading [56]. This variation is dependent on the influence the hydrophilic GO has on the rate of solvent de-mixing and final deposition of the filler within the membrane polymer matrix. In this case, the combination of porous filler and hydrophilic GO support consequently increased water flux by affording the membrane more water transport pathways and increased hydrophilicity that plays a crucial role in membrane performances [3, 11, 57, 89, 97, 106].

In interfacial polymerization (I.P.), the fillers, i.e., ZIF-8@GO, affect the rate of crosslinking between aliphatic/diamine monomer in the aqueous phase and the acid chloride monomer in the organic phase (Fig. 8.10) [37, 38, 89]. Subsequently, the thickness of the thin film is affected, which plays a huge role in membrane performance [37, 38]. It is worth mentioning that the filler effect is usually observed when the filler is dispersed in the organic phase because the diffusion rate of the I.P. process is generally controlled in the organic layer [3, 37, 38]. The SEM images of

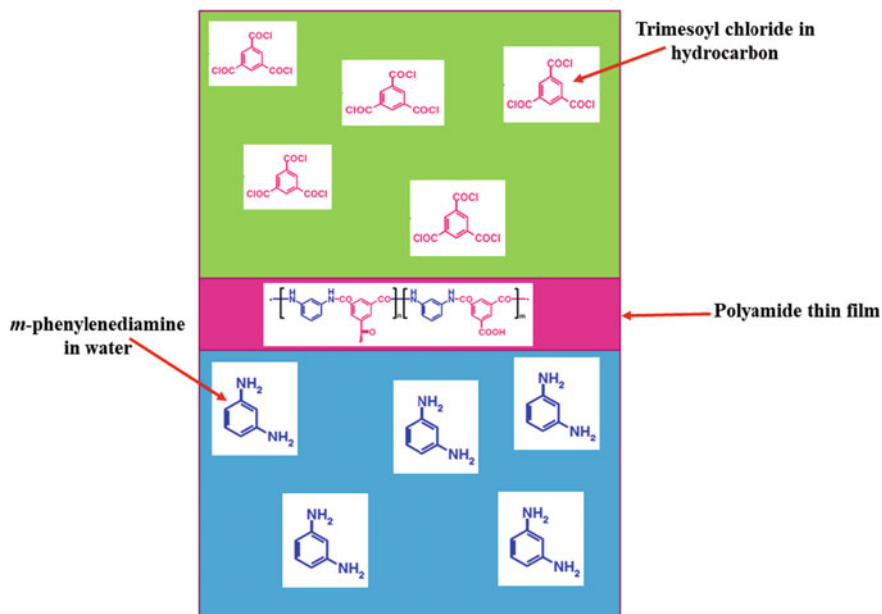


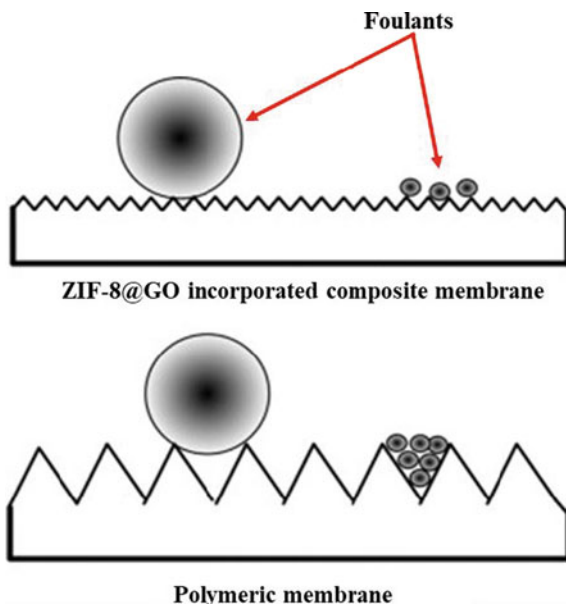
**Fig. 8.10** Representation of the formation of polyamide thin film. Reproduced with permission from (Lau, Ismail, Misdan and Kassim 2012). Copyright 2012 ELSEVIER

thin film composite membranes usually show a thin layer onto the porous substrate, and in some cases, irregular structure is observed, which is assumed to be a result of the growth of initial polyamide clumps caused by the defect in the interface at the beginning of crosslinking.

#### 8.4.1.2 Afm

Recently, the AFM technique has found widespread usage for the study of membrane surfaces. AFM provides atomic-level images and has become a crucial technique for obtaining images of the membrane surface materials. This technique does not require any special sample preparation, as is the case for SEM above. Interestingly, AFM can show three-dimensional images of the surfaces. The quantitative information obtained from AFM provides the microscopic details of the surface structure that is used to obtain a variety of surface roughness parameters as well as in some cases the width of surface pores and surface porosity. Visualizing the effects of fouling and chemical modification on surface morphology is another potential benefit of using this technique. Researchers revealed that the surface roughness of the membrane influence the surface area that is available for contact with foulants [31, 72, 104]. Therefore, surface roughness plays a critical part in establishing the magnitude and

**Fig. 8.11** Representation of the affinity of foulants towards the rougher polymeric membrane and poor affinity towards the smoother ZIF-8@GO modified membrane



nature of membrane surface fouling [31, 72, 104]. Due to the observed correlation between higher surface roughness the increased propensity for surface fouling (Fig. 8.11), great effort into creating membranes with smoother surfaces to minimize fouling has been made. The incorporation of hydrophilic ZIF-8@GO fillers has led to a reduced surface roughness which subsequently enhances fouling resistance of the composite U.F. membrane (Fig. 8.11) [11, 26, 92, 106]. The reduced surface roughness emanates from the affected rate of de-mixing in the phase inversion method and the rate of crosslinking in interfacial polymerization.

#### 8.4.2 Membrane Wettability

Membrane wettability studies usually involve the measurement of contact angles as the primary data, which indicates the degree of wetting when a membrane surface and liquid interact [24, 100]. Small contact angles ( $\theta = 90^\circ$ ) correspond to high wettability, while large contact angles ( $\theta = 90^\circ$ ) correspond to low wettability [24, 100]. The contact angle values are presented in Fig. 8.12. A lower contact angle value signifies the hydrophilic nature of the material, i.e., the high affinity of water molecules toward the membrane substrate [24, 100]. Hydrophilic literally means “water loving” and such materials easily adsorb water molecules due to the presence of active polar functional groups [100]. The higher contact angle indicates the hydrophobic nature of the surface. Hydrophobic materials possessing this characteristic have the opposite

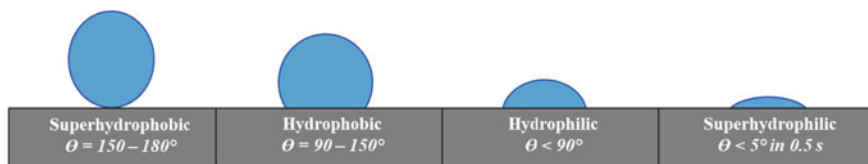


**Fig. 8.12** Demonstration of contact angle formed by a sessile liquid drop on a smooth surface

response to water interaction compared to hydrophilic materials. Hydrophobic materials “water hating” have little or no tendency to interact with water, and water tends to “bead” on their surfaces [24, 100]. The contact angle measurement is in addition also influenced by the physical properties of the membranes such as heterogeneity, surface roughness, pore size, and pore distribution [24]. Suppose a membrane is highly porous due to the incorporation of ZIF-8@GO composite. In that case, the contact angle value may become very low due to the combination of functional groups on GO and porosity afforded by the ZIF-8. In the case where the membrane incorporated only ZIF-8, the overall surface character is less hydrophilic at high filler content. Hence, the observed contact angles are higher compared to its GO analog.

Similarly, the contact angle value of a membrane of higher surface roughness is higher compared to the other membrane of lower surface roughness [11, 56, 57, 89]. Generally, as the contact angle values decreased (membrane become hydrophilic), the flux rate has increased, a behavior observed for composite membranes containing ZIF-8@GO [11, 56, 57, 89]. Hydraulic permeability of the membrane significantly influenced the surface hydrophilicity. These involve the secondary forces of interactions such as dipole–dipole, induced dipole–dipole, Van der Waals forces, electrostatic interaction, hydrogen bonding, etc., between the solution and membrane [24]. This also results in relatively higher fluxes.

### 8.4.3 Water Flux

Water flux is greatly affected by various factors such as membrane hydrophilicity, membrane roughness, membrane pore size, pore density as well as pore distribution. As such, ZIF-8@GO composites have a strong influence on the above-mentioned factors, hence resulting in improved water flux of the composite membrane [11, 56, 57, 89]. Van der Bruggen et al. [89] reported an increase in water flux and permeability owing to the hydrophilic and porous characters of GO and ZIF-8, respectively. This is similar results to our results [56] which was attributed to a decrease in tortuosity owing to the hydrophilic properties of GO and the porous nature of ZIF-8 that allowed for an alternative flow path for water molecules infiltrate through the composite filler (Fig. 8.8). Similarly, Ye et al. and Sun et al. reported a significant increase in water flux and permeation due to the incorporation of UiO-66-NH<sub>2</sub>/GO and UiO-66@GO, respectively [43, 47, 69] in comparison to UiO and GO when used separately. An

increase in flux for the hybrid material is due to the synergistic effect from the MOF and GO; hence more research is focused on using MOF@GO fillers. Furthermore, ZIF-8@GO is extensively used as a filler in membrane technology due to ZIF-8 water stability, the compatibility of the filler with different polymer matrixes as well as selective properties in rejection of various pollutants [11, 56, 89].

#### **8.4.4 Fouling Resistance**

One of the utmost unfavorable problems in the pressure-driven membrane process such as reverse osmosis (R.O), nanofiltration (N.F), ultrafiltration (U.F) and micro-filtration (M.F) is fouling, which hinders the long-term usage and efficiency of the membranes [22, 76]. Fouling is due to the adsorption or deposition of particles, colloids, proteins, macromolecules, salts, etc., at the membrane surface or inside the pores [22, 76]. Generally, fouling is reduced by enhancing the surface hydrophilicity and reducing the surface roughness of the membrane surfaces [22, 76].

Membrane surface hydrophilicity is the affinity of the membrane to attract water molecules towards itself while repelling hydrophobic pollutants [24, 100]. As such, water molecules form a water layer on the hydrophilic membrane surface, reducing the contact between the hydrophobic pollutants and the membrane surface [24, 100]. This phenomenon plays an important role in fouling resistance. For example, Kang et al. and Lee et al. revealed that GO as a filler material increases the hydrophilicity of the composite membranes, subsequently enhancing fouling properties of the composite membranes [40, 98]. Similarly, incorporation of ZIF-8@GO onto polymeric membranes was shown to improve membrane hydrophilicity and therefore increase fouling resistance [11, 56, 89].

The surface roughness of the membrane also plays a crucial role in fouling propensity, as demonstrated by various researchers. As such, Zhang et al. investigated the mechanism and implications of surface roughness and fouling relationship in RO membrane [75]. It was shown that the rougher surface with valleys contributes to an increase in membrane fouling where foulants are trapped within the valleys [75]. Furthermore, it was revealed that the low surface roughness normally has evenly distributed water flux with minimized effects of drag force while making better use of shear force resulting in an increase in fouling resistance [75]. We also reported similar findings, wherein an increase in fouling resistance was observed for membranes with smoother surface roughness in comparison to rougher membrane surfaces [56, 57].

#### **8.4.5 Wastewater Treatment**

Wastewater emanates from municipal discharge, agricultural activities and industrial discharge contaminated by dyes, heavy metals, radioactive nuclides, pesticides as well as miscellaneous and emerging contaminants which ultimately reduce the

quality of drinking water [79]. Consequently, different strategies have been employed for wastewater treatment, such as membrane technology [17], ion exchange [33], and adsorption [79]. These techniques can be utilized to extract valuable constituents for reuse, separate solutes, and ultimately remove all solutes [1, 2]. However, the process depends on the type of technique used, type of contaminant, and material [2, 79]. Herein, the interest is on membrane technology for the removal of solutes from wastewater.

So far, rejection of various contaminants using polymeric membranes is due to size exclusion, depending on the size of the membrane pore and that of the pollutants, electrostatic interaction, hydrogen bonding, etc. [77, 101]. For example, Chang and co-workers investigated the effect of size exclusion in nanofiltration membrane [9]. The results revealed that the pore size of the membranes has much influence on size exclusion compared to cross-flow velocity and the transmembrane pressure [9]. Van Dijk et al. studied the role of electrostatic repulsion between the solute and the membrane at different pH using nanofiltration membranes [88]. On the other hand, Shen et al. explained electrostatic interaction formed between the ion from the pollutants with water molecules forming a shell around the ion, making it difficult for the ions to pass through the membrane [77]. However, rejection percentages using polymeric membranes have been demonstrated to be low.

To enhance rejection % as well as selectivity, ZIF-8, GO, and ZIF-8@GO composite have been used for selective removal of various hazardous pollutants from wastewater [56, 63, 80]. Selective rejection of the pollutants via ZIF-8@GO containing composite membranes were also found to proceed through a number of different mechanisms such as electrostatic interactions, acid–base interactions, hydrogen bonding, stacking/interactions, and hydrophobic interactions (Fig. 8.13) [11, 23, 56, 90]. It has also been observed that sometimes, for a particular selectivity process, multiple interactions might take place to afford 100% of rejection [23].

Jhung et al. reviewed the effect of MOFs selectivity on the adsorptive removal of conventional organic contaminants from wastewater [23]. The authors investigated the possible interactions between the pollutants and the MOFs. Their findings revealed that there is a number of interactions that play a crucial role in different types of adsorption depending on the type of the targeted pollutant and the MOF used. Additionally, Chen and co-workers explored the adsorption of organic and inorganic pollutants using ZIF-8@GO [90]. It was realized that the adsorption mechanisms of ZIF-8@GO towards Pb(II) were complexation and electrostatic attraction, whereas the  $\pi$ – $\pi$  bond was the dominating adsorption mechanism for 1-naphthylamine.

## 8.5 Conclusion

The chapter first described the different types of MOFs as well as their different properties. These are subsequently illustrated with respect to the types of application each MOF is suitable for. It is further indicated that only water-stable MOFs are suitable for application in membrane technology unless the further modification

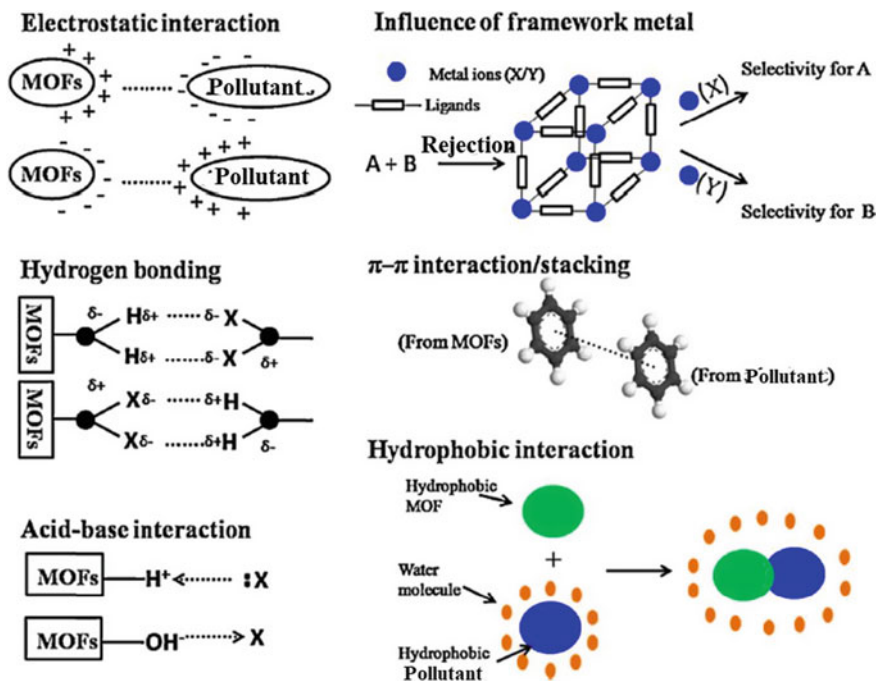


**Fig. 8.13** Possible mechanisms for selective removal of pollutants from wastewater. Reproduced with permission from [23]. Copyright 2015 ELSEVIER

is done to enhance the water stability of the MOF. In addition to water stability, MOFs deemed suitable for membrane technology must possess appropriate pore sizes as well as be compatible with the polymer matrix are other critical considerations. The chapter also showed that proper dispersion of the MOFs in the polymer matrix is enhanced through the use of the carbonaceous dispersant, namely GO. The MOF@GO composite has proven to improve the surface morphology of the membranes by modulating pore density, reducing surface roughness, and enhancing surface hydrophilicity. These improved surface characteristics result in enhanced membrane performance, i.e., high water flux due to synergistic effect from porous MOF and hydrophilic GO, rejection efficiency of the membranes is also influenced by the use of hybrid material; as such, multi rejection mechanisms is realized, resulting in the selectivity of the pollutants. Ultimately, the chapter has demonstrated that the use of a zeolitic organic framework coupled with graphene oxide is currently providing enhanced characteristics in the membrane for water treatment and thus offers a promising future role in the field.



## References

1. M.A. Abdel-fatah, Nanofiltration systems and applications in wastewater treatment: review article. *Ain Shams Eng. J.* **9**(4), 3077–3092 (2018). <https://doi.org/10.1016/j.asej.2018.08.001>
2. N. Abdullah et al., Recent trends of heavy metal removal from water/wastewater by membrane technologies. *J. Ind. Eng. Chem.* (2019). <https://doi.org/10.1016/j.jiec.2019.03.029>
3. N. Abdullah et al., Insights into metal-organic frameworks-integrated membranes for desalination process: a review. *Desalination* **500**, 114867 (2021). <https://doi.org/10.1016/j.desal.2020.114867>
4. H. Amrouche et al., Prediction of thermodynamic properties of adsorbed gases in zeolitic imidazolate frameworks. *RSC Adv.* **2**(14), 6028–6035 (2012). <https://doi.org/10.1039/c2ra00025c>
5. R. Banerjee, High-throughput synthesis of zeolitic imidazolate frameworks and application to CO<sub>2</sub> capture. *Science* **319**, 939–944 (2008). <https://doi.org/10.1126/science.1152516>
6. L. Bellarosa et al., On the mechanism behind the instability of isoreticular metal-organic frameworks (IRMOFs) in humid environments. *Chem. Eur. J.* **18**(39), 12260–12266 (2012). <https://doi.org/10.1002/chem.201201212>
7. S. Bhattacharjee et al., Zeolitic imidazolate frameworks: synthesis, functionalization, and catalytic/adsorption applications. *Catal. Surv. Asia* **18**(4), 101–127 (2014). <https://doi.org/10.1007/s10563-014-9169-8>
8. J.H. Cavka et al., A new zirconium inorganic building brick forming metal organic frameworks with exceptional stability. *J. Am. Chem. Soc.* **130**(42), 13850–13851 (2008). <https://doi.org/10.1021/ja8057953>
9. E. Chang et al., A simplified method for elucidating the effect of size exclusion on nanofiltration membranes. *Sep. Purif. Technol.* **85**, 1–7 (2012). <https://doi.org/10.1016/j.seppur.2011.05.002>
10. J. Chen et al., A facile synthesis for uniform tablet-like TiO<sub>2</sub>/C derived from materials of institut lavoisier-125(Ti) (MIL-125(Ti)) and their enhanced visible light-driven photodegradation of tetracycline. *J. Colloid Interface Sci.* **571**, 275–284 (2020). <https://doi.org/10.1016/j.jcis.2020.03.055>
11. X. Dai et al., Zeolitic Imidazole Framework/graphene oxide hybrid functionalized poly(lactic acid) electrospun membranes: a promising environmentally friendly water treatment material. *ACS Omega* **3**(6), 6860–6866 (2018). <https://doi.org/10.1021/acsomega.8b00792>
12. C. Duan et al., Water-based routes for synthesis of metal-organic frameworks: a review. *Sci. China Mater.* **63**(5), 667–685 (2020). <https://doi.org/10.1007/s40843-019-1264-x>
13. W.A. El-Mehalmey et al., Strong interplay between polymer surface charge and MOF cage chemistry in mixed-matrix membrane for water treatment applications. *ACS Appl. Mater. Interfaces.* **12**(24), 27625–27631 (2020). <https://doi.org/10.1021/acsami.0c06399>
14. A. Elrasheedy et al., Metal organic framework based polymer mixed matrix membranes: review on applications in water purification. *Membranes* **9**(7) (2019). <https://doi.org/10.3390/membranes9070088>
15. S.K. Elsaidi et al., Flexibility in metal-organic frameworks: a fundamental understanding. *Coord. Chem. Rev.* **358**, 125–152 (2018). <https://doi.org/10.1016/j.ccr.2017.11.022>
16. J.F. Eubank et al., Porous, rigid metal(III)-carboxylate metal-organic frameworks for the delivery of nitric oxide. *APL Mater.* **2**(12) (2014). <https://doi.org/10.1063/1.4904069>
17. E.O. Ezugbe, S. Rathilal, Membrane technologies in wastewater treatment: a review. *Membranes* (2020). <https://doi.org/10.3390/membranes10050089>
18. F. Millange, G.F. Christian Serre, Synthesis, structure determination and properties of MIL-53as and MIL-53ht: the first Cr(III) hybrid inorganic-organic microporous solids: Cr(III)(OH)·{O<sub>2</sub>C–C<sub>6</sub>H<sub>4</sub>–CO<sub>2</sub>}·{HO<sub>2</sub>C–C<sub>6</sub>H<sub>4</sub>–CO<sub>2</sub>H}<sub>x</sub>. *R. Soc. Chem.* **601**(2), 51–56 (2000)
19. J.M. Gohil, R.R. Choudhury, Introduction to nanostructured and nano-enhanced polymeric membranes: preparation, function, and application for water purification. *Nanoscale Mater. Water Purif.*. Elsevier Inc (2019). <https://doi.org/10.1016/B978-0-12-813926-4.00038-0>

20. Q. Gu et al., 'Metal-organic frameworks (MOFs)-boosted filtration membrane technology for water sustainability. *APL Mater.* **8**(4) (2020). <https://doi.org/10.1063/5.0002905>
21. G.R. Guillen et al., Preparation and characterization of membranes formed by nonsolvent induced phase separation: a review. *Ind. Eng. Chem. Res.* **50**(7), 3798–3817 (2011). <https://doi.org/10.1021/ie101928r>
22. W. Guo, H.H. Ngo, J. Li, A mini-review on membrane fouling. *Biores. Technol.* **122**, 27–34 (2012). <https://doi.org/10.1016/j.biortech.2012.04.089>
23. Z. Hasan, S.H. Jung, Removal of hazardous organics from water using metal-organic frameworks (MOFs): plausible mechanisms for selective adsorptions. *J. Hazard. Mater.* **283**, 329–339 (2015). <https://doi.org/10.1016/j.jhazmat.2014.09.046>
24. R.S. Hebbar, A.M. Isloor, A.F. Ismail, *Contact Angle Measurements, Membrane Characterization*. Elsevier B.V (2017). <https://doi.org/10.1016/B978-0-444-63776-5.00012-7>
25. S. Hu et al., Effects of monocarboxylic acid additives on synthesizing metal-organic framework NH2-MIL-125 with controllable size and morphology. *Cryst. Growth Des.* **17**(12), 6586–6595 (2017). <https://doi.org/10.1021/acs.cgd.7b01250>
26. A. Huang, B. Feng, Facile synthesis of PEI-GO@ZIF-8 hybrid material for CO2 capture. *Int. J. Hydrogen Energy* **43**(4), 2224–2231 (2018). <https://doi.org/10.1016/j.ijhydene.2017.12.070>
27. N.A. Ibrahim et al., 'Development of polyvinylidene fluoride (PVDF)-ZIF-8 membrane for wastewater treatment, in *IOP Conference Series: Earth and Environmental Science* (2018). <https://doi.org/10.1088/1755-1315/140/1/012021>
28. T. Islamoglu et al., From transition metals to lanthanides to actinides: metal-mediated tuning of electronic properties of isostructural metal-organic frameworks. *Inorg. Chem.* **57**(21), 13246–13251 (2018). <https://doi.org/10.1021/acs.inorgchem.8b01748>
29. F. Israr et al., Scope of various solvents and their effects on solvothermal synthesis of Ni-BTC. *Quim. Nova* **39**(6), 669–675 (2016). <https://doi.org/10.5935/0100-4042.20160068>
30. C. Janiak, J.K. Vieth, MOFs, MILs and more: Concepts, properties and applications for porous coordination networks (PCNs). *New J. Chem.* **34**(11), 2366–2388 (2010). <https://doi.org/10.1039/c0nj00275e>
31. D. Johnson, N. Hilal, *Atomic Force Microscopy (AFM), Membrane Characterization*. Elsevier B.V (2017). <https://doi.org/10.1016/B978-0-444-63776-5.00007-3>
32. M. Kadhom, B. Deng, Metal-organic frameworks (MOFs) in water filtration membranes for desalination and other applications. *Appl. Mater. Today* **11**, 219–230 (2018). <https://doi.org/10.1016/j.apmt.2018.02.008>
33. N. Kansara et al., Wastewater treatment by ion exchange method: a review of past and recent researches. *Environ. Sci.-Indian J.* **12**(4), 143–150 (2016). <http://www.tsijournals.com/articles/wastewater-treatment-by-ion-exchange-method-a-review-of-past-and-recent-researches.pdf>
34. M.J. Katz et al., A facile synthesis of UiO-66, UiO-67 and their derivatives. *Chem. Commun.* **49**(82), 9449–9451 (2013). <https://doi.org/10.1039/c3cc46105j>
35. N.A. Khan, Z. Hasan, S.H. Jung, Beyond pristine metal-organic frameworks: preparation and application of nanostructured, nanosized, and analogous MOFs. *Coord. Chem. Rev.* **376**, 20–45 (2018). <https://doi.org/10.1016/j.ccr.2018.07.016>
36. K. Kumar et al., *Inorganica chimica acta* a review on contemporary metal – organic framework materials. *Inorg. Chim. Acta* **446**, 61–74 (2016). <https://doi.org/10.1016/j.ica.2016.02.062>
37. W.J. Lau et al., 'A recent progress in thin film composite membrane : a review' **287**, 190–199 (2012). <https://doi.org/10.1016/j.desal.2011.04.004>
38. W.J. Lau et al., A recent progress in thin film composite membrane: a review. *Desalination* **287**, 190–199 (2012). <https://doi.org/10.1016/j.desal.2011.04.004>
39. J. Lee et al., Metal – organic framework-based porous matrix membranes for improving mass transfer in forward osmosis membranes. *J. Membr. Sci.* **492**, 392–399 (2015). <https://doi.org/10.1016/j.memsci.2015.06.003>
40. J. Lee et al., Graphene oxide nanoplatelets composite membrane with hydrophilic and antifouling properties for wastewater treatment. *J. Membr. Sci.* **448**, 223–230 (2013). <https://doi.org/10.1016/j.memsci.2013.08.017>

41. T.H. Lee et al., High-performance polyamide thin-film nanocomposite membranes containing ZIF-8/CNT hybrid nanofillers for reverse osmosis desalination. *Ind. Eng. Chem. Res.* **59**(12), 5324–5332 (2020). <https://doi.org/10.1021/acs.iecr.9b04810>
42. S. Leubner et al., Solvent impact on the properties of benchmark metal-organic frameworks: acetonitrile-based synthesis of CAU-10, Ce-UiO-66, and Al-MIL-53. *Chem. Eur. J.* **26**(17), 3877–3883 (2020). <https://doi.org/10.1002/chem.201905376>
43. J. Li et al., The performance of UiO-66-NH<sub>2</sub>/graphene oxide (GO) composite membrane for removal of differently charged mixed dyes' *Chemosphere* **237**, 124517 (2019). <https://doi.org/10.1016/j.chemosphere.2019.124517>
44. J. Li et al., Metal-organic framework membranes for wastewater treatment and water regeneration. *Coord. Chem. Rev.* **404**, 213116 (2020). <https://doi.org/10.1016/j.ccr.2019.213116>
45. N. Li et al., Governing metal – organic frameworks towards high stability 8501–8513 (2016). <https://doi.org/10.1039/c6cc02931k>
46. T. Li et al., Double layer MOFs M-ZIF-8@ZIF-67: The adsorption capacity and removal mechanism of fipronil and its metabolites from environmental water and cucumber samples. *J. Adv. Res.* **24**, 159–166 (2020). <https://doi.org/10.1016/j.jare.2020.03.013>
47. W. Li, Metal–organic framework membranes: production, modification, and applications. *Prog. Mater. Sci.* **100**, 21–63 (2019). <https://doi.org/10.1016/j.pmatsci.2018.09.003>
48. R. Lin et al., Metal organic framework based mixed matrix membranes: an overview on filler/polymer interfaces. *J. Mater. Chem. A* **6**(2), 293–312 (2018). <https://doi.org/10.1039/c7ta07294e>
49. R.B. Lin et al., Microporous metal-organic framework materials for gas separation. *Chem* **6**(2), 337–363 (2020). <https://doi.org/10.1016/j.chempr.2019.10.012>
50. M. Liu et al., Formation of microporous polymeric membranes via thermally induced phase separation: a review. *Front. Chem. Sci. Eng.* **10**(1), 57–75 (2016). <https://doi.org/10.1007/s11705-016-1561-7>
51. Liu, X. (2020) 'Metal-organic framework UiO-66 membranes', 14(2), 216–232.
52. Y. Liu et al., Effect of metal-ligand ratio on the CO<sub>2</sub> adsorption properties of Cu-BTC metal-organic frameworks. *RSC Adv.* **8**(62), 35551–35556 (2018). <https://doi.org/10.1039/c8ra07774f>
53. J. Ma, D. Ping, X. Dong, 'Recent developments of graphene oxide-based membranes: A review'. *Membranes* **7**(3) (2017). <https://doi.org/10.3390/membranes7030052>
54. Z. Mai, D. Liu, Synthesis and applications of isoreticular metal-organic frameworks IRMOF-n (n = 1, 3, 6, 8). *Cryst. Growth Des.* **19**(12), 7439–7462 (2019). <https://doi.org/10.1021/acs.cgd.9b00879>
55. T.A. Makhetha, R.M. Moutloali, Antifouling properties of Cu(tpa)@GO/PES composite membranes and selective dye rejection. *J. Membr. Sci.* **554**(January), 195–210 (2018). <https://doi.org/10.1016/j.memsci.2018.03.003>
56. T.A. Makhetha, R.M. Moutloali, Stable zeolitic imidazolate framework-8 supported onto graphene oxide hybrid ultrafiltration membranes with improved fouling resistance and water flux. *Chem. Eng. J. Adv.* **1**, 100005 (2020). <https://doi.org/10.1016/j.cej.2020.100005>
57. T.A. Makhetha, R.M. Moutloali, Incorporation of a novel Ag–Cu@ZIF-8@GO nanocomposite into polyethersulfone membrane for fouling and bacterial resistance. *J. Membr. Sci.* **618**, 118733 (2021). <https://doi.org/10.1016/j.memsci.2020.118733>
58. M. Miculescu et al., Graphene-based polymer nanocomposite membranes: a review. *Polym. Adv. Technol.* **27**(7), 844–859 (2016). <https://doi.org/10.1002/pat.3751>
59. E.D. Miensah et al., Zeolitic imidazolate frameworks and their derived materials for sequestration of radionuclides in the environment: a review. *Crit. Rev. Environ. Sci. Technol.* **50**(18), 1874–1934 (2020). <https://doi.org/10.1080/10643389.2019.1686946>
60. F. Millange, R.I. Walton, MIL-53 and its isoreticular analogues: a review of the chemistry and structure of a prototypical flexible metal-organic framework. *Isr. J. Chem.* **58**(9), 1019–1035 (2018). <https://doi.org/10.1002/ijch.201800084>

61. A.S. Munn et al., M(ii) (M = Mn Co, Ni) variants of the MIL-53-type structure with pyridine-N-oxide as a co-ligand. *CrystEngComm* **15**(45), 9679–9687 (2013). <https://doi.org/10.1039/c3ce41268g>
62. M.A. Mutalib et al., Chapter 9 - Scanning Electron Microscopy (SEM); and Energy-Dispersive X-Ray (EDX); Spectroscopy, Membrane Characterization, Elsevier B.V (2017). <https://doi.org/10.1016/B978-0-444-63776-5.00009-7>
63. J. Nambikkattu, J. Jose, N.J. Kaleekkal, Materials today: proceedings tailoring the performance of thin-film composite membrane using ZIF-8 for wastewater treatment. *Mater. Today: Proc.* **47**, 1394–1399 (2021). <https://doi.org/10.1016/j.matpr.2021.02.619>
64. N.I.M. Nawi et al., Development of hydrophilic PVDF membrane using vapour induced phase separation method for produced water treatment. *Membranes* **10**(6), 1–17 (2020). <https://doi.org/10.3390/membranes10060121>
65. K. Noh, J. Lee, J. Kim, Compositions and structures of zeolitic imidazolate frameworks. *Isr. J. Chem.* **58**(9), 1075–1088 (2018). <https://doi.org/10.1002/ijch.201800107>
66. N.A.H.M. Nordin et al., Aqueous room temperature synthesis of zeolitic imidazole framework 8 (ZIF-8) with various concentrations of triethylamine. *RSC Adv.* **4**(63), 33292–33300 (2014). <https://doi.org/10.1039/c4ra03593c>
67. M. Oveisi, M.A. Asli, N.M. Mahmoodi, MIL-Ti metal-organic frameworks (MOFs) nanomaterials as superior adsorbents: synthesis and ultrasound-aided dye adsorption from multicomponent wastewater systems. *J. Hazard. Mater.* **347**, 123–140 (2018). <https://doi.org/10.1016/j.jhazmat.2017.12.057>
68. Y. Pan et al., Core-Shell ZIF-8@ZIF-67-derived CoP nanoparticle-embedded N-doped carbon nanotube hollow polyhedron for efficient overall water splitting. *J. Am. Chem. Soc.* **140**(7), 2610–2618 (2018). <https://doi.org/10.1021/jacs.7b12420>
69. J. Pang et al., Exploring the sandwich antibacterial membranes based on UiO-66/graphene oxide for forward osmosis performance. *Carbon* **144**, 321–332 (2019). <https://doi.org/10.1016/j.carbon.2018.12.050>
70. R. Sabouni, H. Kazemian, S. Rohani, Carbon dioxide capturing technologies: a review focusing on metal organic framework materials (MOFs). *Environ. Sci. Pollut. Res.* **21**(8), 5427–5449 (2014). <https://doi.org/10.1007/s11356-013-2406-2>
71. R.R. Salunkhe, Y.V. Kaneti, Y. Yamauchi, Metal-organic framework-derived nanoporous metal oxides toward supercapacitor applications: progress and prospects. *ACS Nano* **11**(6), 5293–5308 (2017). <https://doi.org/10.1021/acsnano.7b02796>
72. Sataloff, R. T., Johns, M. M. and Kost, K. M. (1990) *Synthetic Membranes for Membrane Processes*.
73. G.E.M. Schukraft et al., Isoreticular expansion of polyMOFs achieves high surface area materials. *Chem. Commun.* **53**(77), 10684–10687 (2017). <https://doi.org/10.1039/c7cc04222a>
74. R. Seetharaj et al., Dependence of solvents, pH, molar ratio and temperature in tuning metal organic framework architecture. *Arab. J. Chem.* **12**(3), 295–315 (2019). <https://doi.org/10.1016/j.arabjc.2016.01.003>
75. C. Shang, D. Pranantyo, S. Zhang, Understanding the roughness-fouling relationship in reverse osmosis: mechanism and implications. *Environ. Sci. Technol.* **54**(8), 5288–5296 (2020). <https://doi.org/10.1021/acs.est.0c00535>
76. Q. She et al., Membrane fouling in osmotically driven membrane processes: a review. *J. Membr. Sci.* **499**, 201–233 (2016). <https://doi.org/10.1016/j.memsci.2015.10.040>
77. M. Shen, S. Ketten, R.M. Lueptow, Rejection mechanisms for contaminants in polymeric reverse osmosis membranes (2016), pp. 36–47
78. G. Skorupskii et al., Efficient and tunable one-dimensional charge transport in layered lanthanide metal-organic frameworks. *ChemRxiv* (2018), pp. 1–23. <https://doi.org/10.26434/chemrxiv.7253192>
79. N.H. Solangi et al., ‘n Pr pr oo f’. *J. Hazard. Mater.* 125848 (2021). <https://doi.org/10.1016/j.jhazmat.2021.125848>

80. Y. Song et al., Journal of Water Process Engineering Efficient removal and fouling-resistant of anionic dyes by nano filtration membrane with phosphorylated chitosan modified graphene oxide nanosheets incorporated selective layer'. J. Water Process. Eng. **34**(November 2019), 101086 (2020). <https://doi.org/10.1016/j.jwpe.2019.101086>
81. J. Spencer, The sustainable development goals. Des. Glob. Chall. Goals **12**, 25 (2021). <https://doi.org/10.4324/9781003099680-3>
82. D. Sun et al., Pore-environment engineering in multifunctional metal-organic frameworks. Chin. J. Chem. **38**, 509–524 (2020). <https://doi.org/10.1002/cjoc.201900493>
83. X.M. Tan, D. Rodrigue, 'a review on porous polymeric membrane preparation. Part I: production techniques with polysulfone and poly (Vinylidene Fluoride). Polymers **11**(8) (2019)
84. D.J. Tranchemontagne, J.R. Hunt, O.M. Yaghi, Room temperature synthesis of metal-organic frameworks: MOF-5, MOF-74, MOF-177, MOF-199, and IRMOF-0. Tetrahedron **64**(36), 8553–8557 (2008). <https://doi.org/10.1016/j.tet.2008.06.036>
85. B. Tylkowski, I. Tsibranska, Overview of main techniques used for membrane characterization. J. Chem. Technol. Metall. **50**(1), 3–12 (2015)
86. United Nations (2020) 'The Sustainable Development Goal 6 Global Acceleration Framework', 17. Available at: [www.unwater.org/publications/the-sdg-6-global-acceleration-framework/](http://www.unwater.org/publications/the-sdg-6-global-acceleration-framework/).
87. K. Ventura et al., Superparamagnetic MOF@GO Ni and Co based hybrid nanocomposites as efficient water pollutant adsorbents. Sci. Total Environ. **738**, 139213 (2020). <https://doi.org/10.1016/j.scitotenv.2020.139213>
88. A.R.D. Verliefde et al., The role of electrostatic interactions on the rejection of organic solutes in aqueous solutions with nanofiltration **322**, 52–66 (2008). <https://doi.org/10.1016/j.memsci.2008.05.022>
89. J. Wang et al., Zeolitic Imidazolate framework/graphene oxide hybrid nanosheets functionalized thin film nanocomposite membrane for enhanced antimicrobial performance. ACS Appl. Mater. Interfaces **8**(38), 25508–25519 (2016). <https://doi.org/10.1021/acsami.6b06992>
90. J. Wang et al., Journal of Colloid and Interface Science Exploration of the adsorption performance and mechanism of zeolitic imidazolate framework-8 @ graphene oxide for Pb ( II ) and 1-naphthylamine from aqueous solution. J. Colloid Interface Sci. **542**, 410–420 (2019). <https://doi.org/10.1016/j.jcis.2019.02.039>
91. Q. Wang et al., Recent advances in MOF-based photocatalysis: environmental remediation under visible light. Inorg. Chem. Front. **7**, 300–339 (2020). <https://doi.org/10.1039/c9qi01120j>
92. N. Wei et al., Fabrication of an amine-modified ZIF-8@GO membrane for high-efficiency adsorption of copper ions. New J. Chem. **43**(14), 5603–5610 (2019). <https://doi.org/10.1039/C8NJ06521G>
93. J. Winarta et al., A decade of uio-66 research: a historic review of dynamic structure, synthesis mechanisms, and characterization techniques of an archetypal metal-organic framework. Cryst. Growth Des. **20**(2), 1347–1362 (2020). <https://doi.org/10.1021/acs.cgd.9b00955>
94. World Health Organization and UN-Habitat, *Progress on wastewater treatment - Piloting the monitoring mehtodology and intial findings for SDG indicator 6.3.1, Guidelines on Sanitation and Health* (2018)
95. M.X. Wu et al., Core-Shell MOFs@MOFs: diverse designability and enhanced selectivity. ACS Appl. Mater. Interfaces **12**(49), 54285–54305 (2020). <https://doi.org/10.1021/acsami.0c16428>
96. W. Xuan et al., Mesoporous metal-organic framework materials. Chem. Soc. Rev. **41**(5), 1677–1695 (2012). <https://doi.org/10.1039/c1cs15196g>
97. L. Yang, Z. Wang, J. Zhang, ( 'Zeolite imidazolate framework hybrid nanofiltration (NF) membranes with enhanced permselectivity for dye removal.' J. Membr. Sci. **532**, 76–86 (December 2016) (2017). <https://doi.org/10.1016/j.memsci.2017.03.014>
98. Y. Yoon et al., Comparing graphene oxide and reduced graphene oxide as blending materials for polysulfone and polyvinylidene difluoride membranes. Appl. Sci. (Switzerland) **10**(6) (2020). <https://doi.org/10.3390/app10062015>

99. Q. Yuan, G. Zhu, A review on metal organic frameworks (MOFs) modified membrane for remediation of water pollution. *Environ. Eng. Res.* **26**, 3–2 (2020). <https://doi.org/10.4491/eer.2019.435>
100. Y. Yuan, T.R. Lee, *Contact Angle and Wetting Properties* (2013). <https://doi.org/10.1007/978-3-642-34243-1>
101. M. Zahid et al., *Role of Polymeric Nanocomposite Membranes for the Removal of Textile Dyes from Wastewater* (Elsevier Inc., Aquanotechnology, 2021). <https://doi.org/10.1016/B978-0-12-821141-0.00006-9>
102. G. Zhan, H.C. Zeng, Alternative synthetic approaches for metal-organic frameworks: transformation from solid matters. *Chem. Commun.* **53**(1), 72–81 (2017). <https://doi.org/10.1039/c6cc07094a>
103. W.H. Zhang et al., Graphene oxide membranes with stable porous structure for ultrafast water transport. *Nat. Nanotechnol.* (2021). <https://doi.org/10.1038/s41565-020-00833-9>
104. Z. Zhong et al., Membrane surface roughness characterization and its influence on ultrafine particle adhesion. *Sep. Purif. Technol.* **90**, 140–146 (2012). <https://doi.org/10.1016/j.seppur.2011.09.016>
105. H. Zhou et al., Stable Metal-Organic Frameworks: Design, Synthesis, and Applications. *Adv. Mater.* **30**, 1704303 (2018). <https://doi.org/10.1002/adma.201704303>
106. T. Zhu et al., ZIF-8@GO composites incorporated polydimethylsiloxane membrane with prominent separation performance for ethanol recovery. *J. Membr. Sci.* **598**, 117681 (2020). <https://doi.org/10.1016/j.memsci.2019.117681>